Supplemental
Filtering Environment Illumination for Interactive Physically-Based Rendering in Mixed Reality

Paper1010

April 7, 2015

1 Two-mode Sampling Algorithm

We propose a two-mode path-tracer that traces OptiX rays to intersect only virtual geometry, and screen-space rays to intersect only real geometry. Our sampling algorithm is explained in Algorithm 1. For brevity, we omit obvious function arguments. Position and normal are abbreviated to 'pos' and 'n'; real and virtual quantities are separated with suffixes '_r' and '_v' respectively.

The main blocks in the code are explained below:
Lines 3-12: The outer loop consists of 4 samples per pixel (spp) anti-aliasing, and we determine whether a real or a virtual object is visible at the current sample and update the mask M.
Line 13: This loop computes 4 secondary samples for each of the 4 primary samples, so we compute a total of 16 spp for each of direct and indirect illumination.
Lines 14-25: For direct illumination, we importance sample the environment map, as this gives the least amount of noise for very little overhead. In line 15, an environment map importance sample is obtained, and in lines 18-19, the functions *trace_optix_sray* and *trace_ss_sray* return hit distances (-1 if no hit) for OptiX and screen-space shadow rays respectively.
Lines 26-40: For indirect illumination, we sample the cosine hemisphere for diffuse surfaces (real and virtual) and a Phong lobe for glossy surfaces (virtual only). Line 27 samples the BRDF to produce a sampling direction, and in lines 28-29, *trace_optix_iray* and *trace_ss_iray* return the indirect radiance and hit distance for OptiX and screen-space indirect rays respectively. In line 28, for screen-space rays, radiance from the secondary hit is computed by L_{cam} image look-up. In line 29, radiance from the secondary hit for OptiX rays (that intersect only virtual surfaces) is computed by tracing a secondary shadow ray to an environment map sample.

Although not shown in Algorithm 1, we also save the (average) world location, normal, virtual texture k_V. We also record the minimum hit distance for direct and indirect illumination; these are required for filtering. Since texture is multiplied with irradiance after filtering, we require the approximation $\langle k \cdot E \rangle \approx \langle k \rangle \cdot \langle E \rangle$, where $\langle\rangle$ denotes the mean of the quantity at a pixel.

This algorithm can be implemented in a single Optix pixel-shader kernel execution. However, Optix kernels are optimized only for ray intersection testing, and thread divergence reduces speed of this one-kernel approach significantly due to the screen-space ray-tracing component. Hence, we implement the algorithm in two passes. A first Optix pass traces only the Optix rays, storing the intersection results in a buffer. A second CUDA pixel shader pass traces the screen-space rays and also combines the result of screen-space and Optix ray-tracing, per lines 21-26 and 32-42 of the pseudo-code.

Algorithm 1

```
for each pixel do
    E_dir_r = E_dir_rv = E_ind_r = E_ind_rv = 0, M = 0
    for i = 1 : 4 do                                                    ▷ Anti-aliasing
        is_real = false
        {pos_v ,n_v ,depth_v} = trace_primary_ray_optix(...)
        {pos_r ,n_r ,depth_r} = real_world_map(...)
        if depth_v = −1 OR depth_r < depth_v then
            is_real = true, M += 0.25
            pos = pos_r, n = n_r
        else
            pos = pos_v, n = n_v
        end if
        for j = 1 : 4 do                                                ▷ Secondary Samples
            // Direct Illumination
            sample = get_importance_sample(...)
            L_env = env_map[sample.xy]
            ray_dir = {pos, sample_to_direction(sample.xy)}
            hit_dist_v = trace_optix_sray(ray_dir)
            hit_dist_r = trace_ss_sray(ray_dir)
            if is_real and hit_dist_r = −1 then
                E_dir_r += L_env * cos_theta / sample.pdf
            end if
            if hit_dist_r = −1 and hit_dist_v = −1 then
                E_dir_rv += L_env * cos_theta / sample.pdf
            end if
            // Indirect Illumination
            ray_ind = {pos, sample_BRDF(...)}
            {hit_dist_v, L_ind_v} = trace_optix_iray(ray_ind)
            {hit_dist_r, L_ind_r} = trace_ss_iray(ray_ind)
            if hit_dist_r > 0 and hit_dist_v> 0 then
                if hit_dist_r > hit_dist_v then
                    E_ind_rv += L_ind_v
                else
                    E_ind_rv += L_ind_r
                end if
            end if
            // Cases where dist= −1 not shown
            if is_real and hit_dist_r > 0 then
                E_ind_r += L_ind_r
            end if
        end for
    end for
    E_{dir|ind}_{r|rv} /= 16 // normalize quantities
end for
```

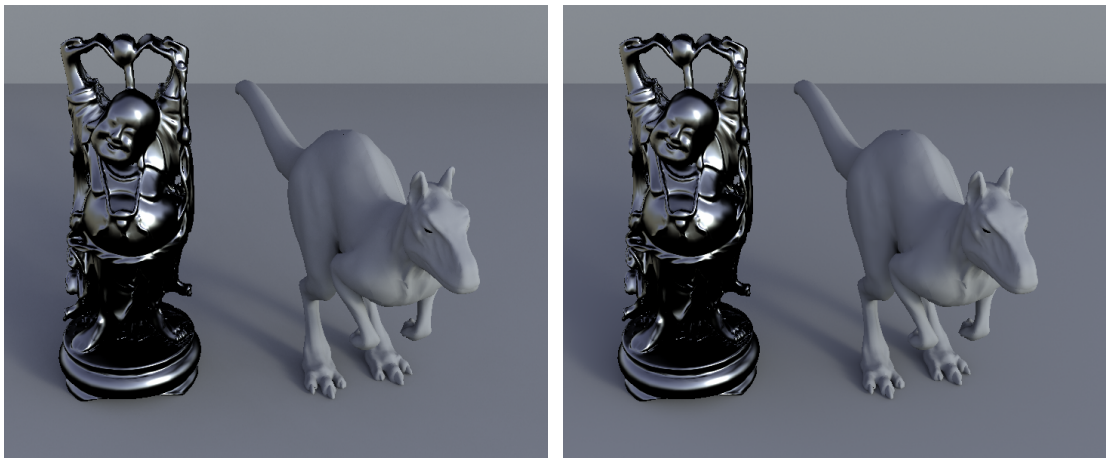

Our Pre-computed Importance Sampling, 1024 spp | BRDF Importance Sampling, 4096 spp (Ground Truth)

Figure 1

1.1 Comparing our Importance Sampling to Ground Truth

As explained in Sec 5.2 in the paper, we pre-compute 4096 importance samples and render the image by choosing samples from this pre-computed set. In Fig. 1, we compare a 1024 spp image rendered with the pre-computed importance samples, to a ground truth image with 4096 spp BRDF importance sampling. There is no visual difference, and the numeric (RMS, per channel) error is 10^{-5}.

2 Derivation of equation 11

Here we prove eqn. 11. Taking the 1D Fourier transform of eqn. 10 gives:

$$\begin{aligned}\hat{E}(\Omega_x) &= \iint L_e(\theta+\kappa x)H(\theta-\theta_{\text{occ}}+\lambda x)f(\theta)e^{-jx\Omega_x}\,d\theta\,dx \\ &= \int\left(\iint L_e(\theta+\kappa x)H(\theta-\theta_{\text{occ}}+\lambda x)\,e^{-jx\Omega_x}e^{-j\theta\Omega_\theta}\,dx\,d\theta\right)\hat{f}(-\Omega_\theta)\,d\Omega_\theta \\ &= \int \hat{G}(\Omega_x,\Omega_\theta)\hat{f}(\Omega_\theta)\,d\Omega_\theta\end{aligned} \tag{1}$$

In the second step, we have used the inverse Fourier transform $f(\theta)=\int \hat{f}(-\Omega_\theta)e^{-j\theta\Omega_\theta}\,d\theta$, and the Fourier transform of f satisfies $\hat{f}(-\Omega_\theta)=\hat{f}(\Omega_\theta)$.

Since both L_e and H are 1D functions sheared along constant slopes, their Fourier transforms are straight lines through the origin. The spectrum of the product $\hat{G}(\Omega_x,\Omega_\theta)$ is then a convolution of two lines of different slopes. We now derive $\hat{G}$ explicitly:

$$\begin{aligned}\hat{G}(\Omega_x,\Omega_\theta) &= \iint L_e(\theta+\kappa x)H(\theta-\theta_{\text{occ}}+\lambda x)\,e^{-jx\Omega_x}e^{-j\theta\Omega_\theta}\,dx\,d\theta \\ &= \mathcal{F}\{L_e(\theta+\kappa x)\} * \mathcal{F}\{H(\theta-\theta_{\text{occ}}+\lambda x)\} \\ &= \iint \hat{L}_e(\omega_\theta)\delta(\omega_x-\kappa\omega_\theta) \\ &\qquad \hat{H}(\Omega_\theta-\omega_\theta)\delta(\Omega_x-\omega_x-\lambda(\Omega_\theta-\omega_\theta))e^{-j\theta_{\text{occ}}\Omega_\theta}\,d\omega_x\,d\omega_\theta\end{aligned} \tag{2}$$

We use the property $\int f(x)\delta(ax-b)dx = f(b/a)/|a|$ to simplify the integral of the product of two delta functions.

$$\int \delta(\omega_x - \kappa\omega_\theta)\delta(\Omega_x - \omega_x - \lambda(\Omega_\theta - \omega_\theta))\,d\omega_x = \delta(\Omega_x - \kappa\omega_\theta - \lambda(\Omega_\theta - \omega_\theta)) \tag{3}$$

Substituting this into eqn. 2 and applying the delta function integral property once again, we get:

$$\begin{aligned}
\hat{G}(\Omega_x, \Omega_\theta) &= e^{-j\theta_{\text{occ}}\Omega_\theta} \int \hat{L}_e(\omega_\theta)\hat{H}(\Omega_\theta - \omega_\theta)\delta(\Omega_x - \kappa\omega_\theta - \lambda(\Omega_\theta - \omega_\theta))\,d\omega_\theta \\
&= \frac{e^{-j\theta_{\text{occ}}\Omega_\theta}}{\lambda - \kappa}\hat{L}_e\left(\frac{-\Omega_x + \lambda\Omega_\theta}{\lambda - \kappa}\right)\hat{H}\left(\Omega_\theta - \frac{-\Omega_x + \lambda\Omega_\theta}{\lambda - \kappa}\right) \\
&= \frac{e^{-j\theta_{\text{occ}}\Omega_\theta}}{\lambda - \kappa}\hat{L}_e\left(-\frac{\Omega_x - \lambda\Omega_\theta}{\lambda - \kappa}\right)\hat{H}\left(\frac{\Omega_x - \kappa\Omega_\theta}{\lambda - \kappa}\right)
\end{aligned} \tag{4}$$

3 Verification of equation 17

In the main paper, Fig. 4 verifies eqn. 13 for a particular diffuse flatland set-up. Here, we provide a similar verfication for eqn. 17, the glossy case. As shown in Fig. 2 below, eqn. 17 over-estimates the true bandwidth, since we simply combine eqn. 16 and eqn. 13. However, this estimate works well for filtering glossy surfaces as shown in Fig. 6.

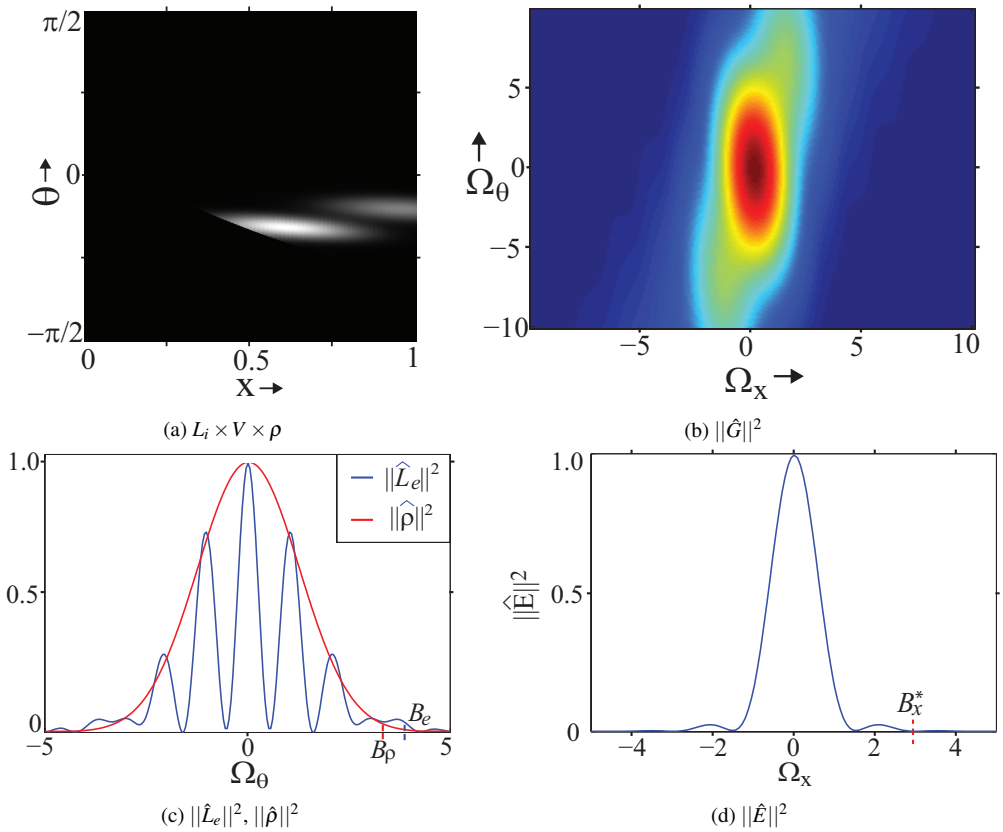

(a) $L_i \times V \times \rho$ (b) $||\hat{G}||^2$

(c) $||\hat{L}_e||^2$, $||\hat{\rho}||^2$ (d) $||\hat{E}||^2$

Figure 2: Verification of eqn. 17 for the simple flatland setup of Fig. 3(c) with a glossy ($n = 32$) surface with $\kappa = 0.5$ and one occluder at $\theta_{\text{occ}} = \pi/4$ and $z = 2$ ($\cos^2\theta_{\text{occ}}/z = 0.25$), under high-frequency illumination. (a) shows the product $L_i \times V(x,\theta)$ for this setup. (b) shows the power spectrum $||\hat{G}||^2$ of (a). In (c) we show the 1D power spectra of L_e and ρ, showing bandlimits $B_e = 4$ and $B_\rho = 3.5$. (d) shows the 1D power spectrum $\hat{E}$ of the surface irradiance, showing the true bandwidth $B_x^* \approx 3$. Eqn. 17 ($B_f = 1$)gives $B_x = 4 + 0.25 \times 12 = 7$. Our estimate is conservative but not tight.